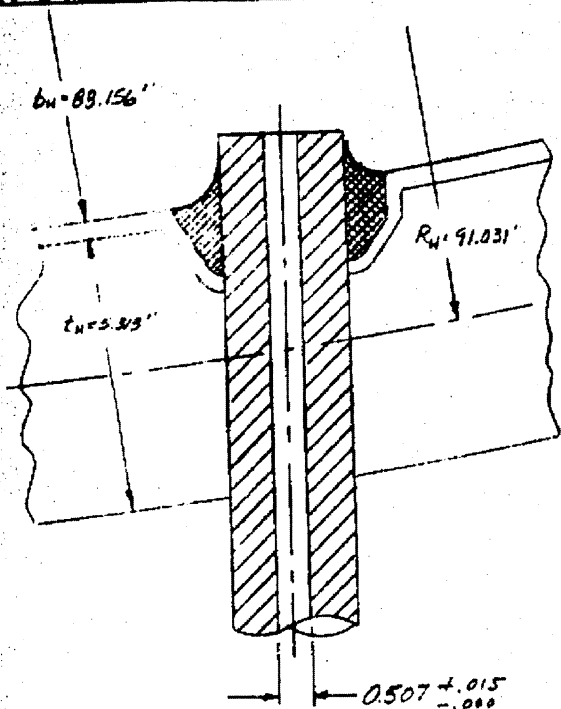


COMBUSTION ENGINEERING, INC.
ENGINEERING DEPARTMENT, CHATTANOOGA, TENN.

NUMBER S-204-P | A 395
SHEET 5 OF 15
DATE 1-11-67 BY COOPER
CHECK DATE 1-11-67 BY CAUDRY
REVISED 4-14-69 BY COOPER

CHARGE NO. _____
DESCRIPTION STRUCTURAL AND FATIGUE ANALYSIS OF
BOTTOM HEAD INSTRUMENTATION PENETRATIONS

5. DETAILED ANALYSIS:
a. SYSTEM GEOMETRY:



MATERIAL:
BOTTOM HEAD — SA-302B
INST. TUBE — INCONEL

DIA. OF HEAD PENETRATION:
 $1.500 \begin{matrix} +0.002 \\ -0.000 \end{matrix}$ INCHES

OUTSIDE DIA. OF INST. TUBE:
 $1.499 \begin{matrix} +0.000 \\ -0.001 \end{matrix}$ INCHES

REF. DWG. E-232-056

b. SYSTEM LOADS:

THE BOTTOM HEAD INSTRUMENTATION PENETRATION AS SHOWN ABOVE WILL BE INVESTIGATED FOR THE FOLLOWING LOADS IN THIS ANALYSIS.

1. DESIGN PRESSURE OF 2.5 KSI AT DESIGN TEMPERATURE OF 650°F
2. THE THERMAL AND PRESSURE TRANSIENTS AS GIVEN IN REF. A

COMBUSTION ENGINEERING, INC.
 ENGINEERING DEPARTMENT, CHATTANOOGA, TENN.
 CHARGE NO. _____

NUMBER 5-201-P | A388
 SHEET 6 OF 15
 DATE 1-11-67 BY GERBELL
 CHECK DATE 1-11-67 BY LAUREL
 REVISED 4-11-67 BY GERBELL

DESCRIPTION STRUCTURAL AND FATIGUE ANALYSIS OF
BOTTOM HEAD INSTRUMENTATION PENETRATIONS

3. DETAILED ANALYSIS:

C. SYSTEM ALLOWABLES:

THE FOLLOWING ALLOWABLE STRESSES ARE BASED ON THE ASME NUCLEAR CODE SECTION III, REFERENCE - 1 AND ARE RELEVANT FOR THIS ANALYSIS:

1. THE AVERAGE PRIMARY STRESS INTENSITY ACROSS A SOLID SECTION SHALL NOT EXCEED S_m AT DESIGN TEMP. (650°F) AND DESIGN PRESSURE (2.5 KSI).
2. THE RANGE OF PRIMARY PLUS SECONDARY STRESS INTENSITY RESULTING FROM MECHANICAL AND THERMAL LOADS SHALL NOT EXCEED $3S_m$ AT ACTUAL METAL TEMP. AND OPERATING PRESSURE.
3. SHOW THAT EACH POINT MEETS THE REQUIREMENTS FOR PEAK STRESS INTENSITY GIVEN IN N-414.5 OF THE ASME CODE SECTION III. THE PROCEDURE WILL BE AS OUTLINED IN N-415.2 OF SECTION III.

A. DESIGN STRING:

CONSIDER THE THICKNESS OF THE INST. TUBE



DESIGN PRESSURE = 2.5 KSI
 DESIGN TEMPERATURE = 650°F
 MATERIAL:
 INCONEL TUBE, $S_m = 29.3 \text{ KSI}$ (FROM CODE CASE 1536)
 $R = 0.261 \text{ in (MAX.)}$
 $t_{ACT} = 0.524 \text{ in}$

FROM N-431 OF SECTION III ASME NUCLEAR CODE:

$$t_{REQD} = \frac{PR}{S_m - 0.5P} = \frac{2.5(0.261)}{29.3 - 1.25} = 0.030 \text{ in} < 0.400 \text{ in ACTUAL THICKNESS; HENCE, CRITERION 5-C-1 IS SATISFIED.}$$

COMBUSTION ENGINEERING, INC.
ENGINEERING DEPARTMENT, CHATTANOOGA, TENN.

NUMBER 5-201-P | A 337

SHEET 7 OF 15

DATE 1-11-67 BY COCKRILL

CHECK DATE 1-11-67 BY LAIDL
REVISED 7-16-67 BY COCKRILL

CHARGE NO. _____

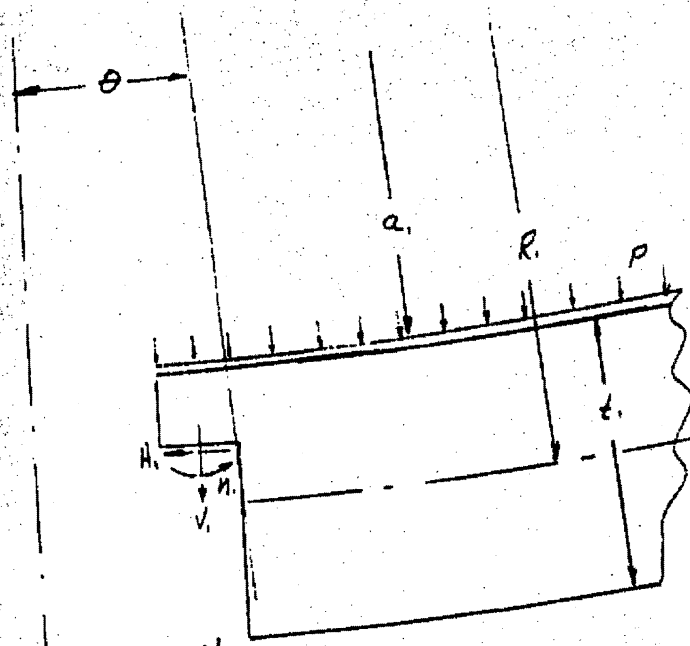
DESCRIPTION STRUCTURAL AND FATIGUE ANALYSIS OF
BOTTOM HEAD INSTRUMENTATION PENETRATIONS

5. DETAILED ANALYSIS:

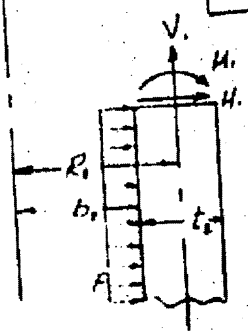
a. INTERACTION ANALYSIS:

1. ANALYTICAL MODEL:

THE ACTUAL STRUCTURE WILL BE APPROXIMATED BY THE FOLLOWING ANALYTICAL MODEL. FOR THE PURPOSE OF THIS ANALYSIS, THE BOTTOM HEAD (ELEMENT -1) WILL BE ASSUMED TO BE A RIGID BODY WITH LOCAL FLEXIBILITY ONLY WHEN CALCULATING THE DISPLACEMENTS DUE TO THE REDUNDANT FORCES. NOTE THAT ELEMENT -1 IS TREATED AS A PERFORATED SHELL WITH AN EFFECTIVE YOUNG'S MODULUS OF E^* AND AN EFFECTIVE POISSON'S RATIO BASED UPON THE LIGAMENT EFFICIENCY WHEN CALCULATING DEFLECTIONS DUE TO PRESSURE.



$R_1 = 91.031$
 $a_1 = 88.156$
 $t_1 = 5.315$
 $\theta_1 = 28.3^\circ$
 $\sin \theta = 0.00925$



$R_2 = 0.505$
 $b_2 = 0.261$
 $t_2 = 0.487$

COMBUSTION ENGINEERING, INC.

ENGINEERING DEPARTMENT, CHATTANOOGA, TENN.

CHARGE NO. _____

STRUCTURAL AND FATIGUE ANALYSIS OF
ROTOR HEAD INSTRUMENTATION PENETRATIONS

NUMBER 5-201-P | A-389

SHEET 8 OF 15

DATE 1-11-67 BY COLEMAN

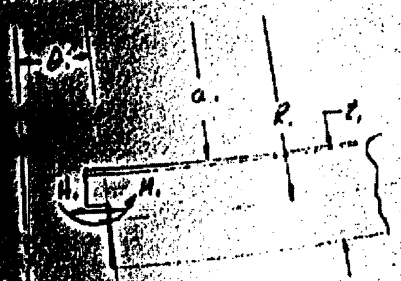
CHECK DATE 1-11-67 BY COLEMAN

3- DETAILED ANALYSIS:

1- INTERACTION ANALYSIS:

2- DEFLECTIONS:

ELEMENT 1:



$$\frac{\Delta \delta}{\Delta \theta}$$

- \$R = 91.031''\$
 - \$a = 18.156''\$
 - \$l = 5.313'\$
 - \$\theta = 28.5^\circ\$
 - \$\frac{R}{l} = 0.88\$
 - \$\gamma = 0.29\$
 - \$\frac{E_2}{E_1} = \frac{E_{steel}}{E_{TiO_2}} = 1.13793\$
- For L.E. = 0.823

DISPLACEMENTS DUE TO REDUNDANT FORCES:

$$E_1 \Delta_1 = -1401(1-\nu^2) \left[\left(\frac{R}{l_2} + \frac{1}{2} \right) \ln \left(\frac{R}{l_2} + \frac{1}{2} \right) - \left(\frac{R}{l_2} - \frac{1}{2} \right) \ln \left(\frac{R}{l_2} - \frac{1}{2} \right) + \frac{1}{2} \right] H_1 + \frac{2.38(1-\nu-2\nu^2)}{l_2} M_1$$

$$= -1.76005 H_1 + 2.36183 M_1$$

$$E_2 \Delta_2 = -\frac{2.38(1-\nu-2\nu^2)}{l_2} H_1 + \frac{6.36(1-\nu^2)}{(l_2)^2} M_1$$

† From Ref. 17

$$= -2.36183 H_1 + 21.07830 M_1$$

DISPLACEMENTS DUE TO PRESSURE:

$$E_1 \delta_1 = \frac{(1-\nu^2)a^2}{2l_1} P \sin \theta \frac{E_2}{E_1} \frac{E_1}{E_1} = \frac{(1-0.29)(18.156)^2}{2(5.313)} P(0.00823) \left(\frac{1}{0.88} \right) (1.13793)$$

$$= 5.52618 P$$

\$E_1 \delta_2 = 0\$

DISPLACEMENTS DUE TO TEMPERATURE

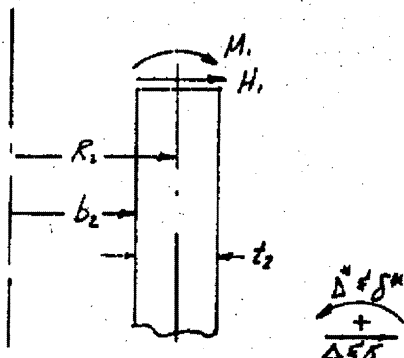
$$E_1 \delta_1 = R_{max} (E\alpha)_1 (T_{m_1} - 70) \frac{E_2}{E_1} = 0.95345 (E\alpha)_1 (T_{m_1} - 70)$$

\$E_1 \delta_2 = 0\$

COMBUSTION ENGINEERING, INC.

ENGINEERING DEPARTMENT, CHATTANOOGA, TENN.

CHARGE NO. _____

NUMBER 5-204-P | A 389SHEET 9 OF 15DATE 1-11-67 BY OSKARDESCRIPTION STRUCTURAL AND FATIGUE ANALYSIS OF
BOTTOM HEAD INSTRUMENTATION PENETRATIONSCHECK DATE 1-11-67 BY CAWOLF
REVISED 1-11-67 BY OSKAR5. DETAILED ANALYSIS:C. INTERACTION ANALYSIS:2. DEFLECTION:ELEMENT 2:

$$R_2 = 0.505''$$

$$b_2 = 0.261''$$

$$t_2 = 0.488''$$

$$\beta^4 = \frac{3(1-\nu^2)}{R^2 t^3} = 44.95109$$

$$\beta^2 = 6.70456$$

$$\beta = 2.58932$$

$$D = \frac{E t^3}{12(1-\nu^2)} = \frac{E}{93.9456}$$

DISPLACEMENTS DUE TO REDUNDANT FORCES:

$$E_2 \Delta_{21} = \frac{E}{2\beta^2 D} H_1 + \frac{E}{2\beta^2 D} M_1 = \underline{2.70631 H_1 + 7.0075 M_1}$$

$$E_2 \Delta_{21}^* = -\frac{E}{2\beta^2 D} H_1 - \frac{E}{\beta D} M_1 = \underline{-7.0075 H_1 - 36.2892 M_1}$$

DISPLACEMENTS DUE TO PRESSURE

$$E_2 S_{21} = \frac{b_2^2}{t_2} \left(\frac{R_2}{b_2} - \frac{\nu}{2} \right) P = \underline{0.24915 P}$$

$$E_2 \delta_{21}^* = \underline{0}$$

DISPLACEMENTS DUE TO TEMPERATURE:

$$E_2 S_{21} = E_2 (E_d)_2 (T_{m_2} - 70) = \underline{0.505 (E_d)_2 (T_{m_2} - 70)}$$

$$E_2 \delta_{21}^* = \underline{0}$$

COMBUSTION ENGINEERING, INC.
 ENGINEERING DEPARTMENT, CHATTANOOGA, TENN.
 CHARGE NO. _____

NUMBER 5-201-P | 1350
 SHEET 10 OF 15
 DATE 1-11-67 BY CECIBELL
 CHECK DATE 1-11-67 BY QUOLP
 REVISU 4-14-67 BY CECIBELL

DESCRIPTION: STRUCTURAL AND FATIGUE ANALYSIS OF BOTTOM HEAD INSTRUMENTATION PENETRATIONS

5. DETAILED ANALYSIS:

1. C. INTERACTION ANALYSIS:

3. CONTINUITY MATRIX AND LOADING VECTORS

FROM CONTINUITY WE HAVE,

$$E_2 \Delta_1 = E_2 \Delta_{21} = E_2 \delta_{21} - E_2 \delta_{11} = -5.27103 D - [0.85345(E\alpha)_1 (T_m - 70) - 0.505(\alpha)_2 (T_m - 70)]$$

$$E_2 \Delta_1^* = E_2 \Delta_{21}^* = E_2 \delta_{21}^* - E_2 \delta_{11}^* = 0$$

LET,

$$W_p + W_T = -5.27103 P - [0.85345(E\alpha)_1 (T_m - 70) - 0.505(E\alpha)_2 (T_m - 70)]$$

IN MATRIX FORM WE HAVE,

$$\begin{bmatrix} -4.46636 & -4.64567 \\ 4.64567 & 57.3575 \end{bmatrix} \begin{bmatrix} H_1 \\ M_1 \end{bmatrix} = \begin{bmatrix} 1 \\ 0 \end{bmatrix} W_p + \begin{bmatrix} 1 \\ 0 \end{bmatrix} W_T$$

4.3. REDUNDANT LOAD VALUES:

SOLVING THE ABOVE MATRIX, WE GET THE FOLLOWING VALUES FOR THE REDUNDANT FORCES,

$$H_1 = -0.24449 (W_p + W_T)$$

$$M_1 = 0.01980 (W_p + W_T)$$

COMBUSTION ENGINEERING, INC.
ENGINEERING DEPARTMENT, CHATTANOOGA, TENN.

NUMBER 5-101-P | A 557

SHEET 11 OF 15

CHARGE NO. _____

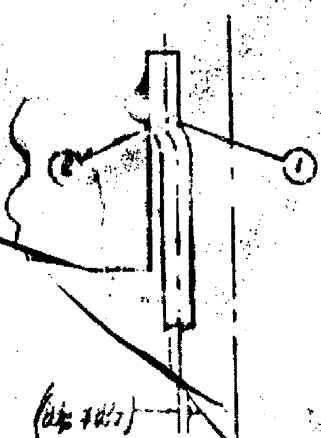
DATE 1-11-67 BY COLEMAN

DESCRIPTION STRUCTURAL AND FATIGUE ANALYSIS OF
ROTOR HEAD IN VIBRATION PENETRATOR

CHECK DATE 1-11-67 BY LAUDLE
REVISED 4-14-68 BY COLEMAN

5. DETAILED ANALYSIS:

1. STRESSES:



TYPICAL DEFLECTION SHAPE DUE TO PRESSURE OR THERMAL CONDITIONS IN WHICH THE TUBE IS COOLER THAN THE VESSEL LOWER HEAD.

STRESSES WILL BE CALCULATED AT THE TWO LOCATIONS AS SHOWN. A STRESS CONCENTRATION FACTOR OF FOUR (4) WILL BE USED AT LOCATION-2 FOR THE FATIGUE EVALUATION AS GIVEN IN N-4624 (d)(3) OF ASME CODE, SECTION III.

LOCATION-1

$$\sigma_r = \frac{6M}{s^2} + \frac{bP}{2s} = \frac{6(0.0190)(W_p + W_r)}{(0.437)^2} + \frac{10.2}{2(0.437)}$$

$$= 0.49886(W_p + W_r) + 0.13521P$$

$$E\Delta_r = 2.70631W_p + 7.001W_r = -0.52292(W_p + W_r)$$

$$\sigma_a = \frac{FEM}{s} + \frac{E\Delta_r}{R_a} + \frac{bP}{s} = \frac{0.31(0.0190)(W_p + W_r)}{(0.437)} + \frac{-0.52292(W_p + W_r)}{(0.437)} + \frac{0.261P}{0.437}$$

$$= 0.4966(W_p + W_r) - 1.0548(W_p + W_r) + 0.5348P$$

LOCATION-2

$$\sigma_r = \frac{6M}{s^2} + \frac{bP}{2s} = -0.49886(W_p + W_r) + 0.13521P$$

$$\sigma_a = \frac{FEM}{s} + \frac{E\Delta_r}{R_a} + \frac{bP}{s} = -0.4966(W_p + W_r) - 1.0548(W_p + W_r) + 0.5348P$$

COMBUSTION ENGINEERING, INC.

ENGINEERING DEPARTMENT, CHATTANOOGA, TENN.

NUMBER 5-204-P | A352

SHEET 12 OF 15

CHARGE NO. _____

DATE _____ BY COCKRILL

DESCRIPTION STRUCTURAL AND FATIGUE ANALYSIS OF
BOILER HEAD INSTRUMENTATION PENETRATIONS

CHECK DATE _____ BY _____

DETAILED ANALYSIS:

STRESS:

STRESS POINT	ANNUAL PRESSURE PSIA	Wp	To °F	(E)1 ksi/yr	To °F	(E)2 ksi/yr	W1	Wp HWT	EM %	EP %	EM %	EP %	
2	0.315	-1.662	70	0.177	99	0.185	2.709	1.087	0	0.04	0	-1.58	0.17
14	2.25	-11.873	512	0.186	547	0.217	-18.144	-30.717	-15.32	0.31	-4.60	31.31	1.20
15	2.25	-11.873	547		547		-23.448	-36.321	-17.62	0.31	-5.29	36.57	1.20
16	2.25	-11.873	547		518		-26.626	-38.499	-19.21	0.31	-5.76	39.86	1.20
17	0.315	-1.662	99	0.178	70	0.180	-1.406	-6.068	-3.03	0.04	-0.91	6.76	0.17
C	2.25	-11.873	547	0.186	555	0.218	-22.326	-34.199	-17.86	0.31	-5.12	35.41	1.20
d	2.25	-11.873	555		547	0.217	-24.718	-36.591	-18.25	0.31	-5.48	37.59	1.20
e	2.14	-11.293	514		575	0.218	-26.218	-37.511	-18.71	0.30	-5.61	38.84	1.14
	2.275	-12.005	574		582	0.218	-25.227	-37.232	-18.57	0.31	-5.57	38.55	1.22
f	2.32	-12.243	584		593	0.219	-23.762	-35.995	-17.46	0.32	-5.39	37.27	1.24
g	2.26	-11.926	584		597	0.219	-23.310	-35.736	-17.58	0.31	-5.27	36.49	1.21
h	2.14	-11.293	584		585	0.218	-24.876	-36.189	-18.09	0.30	-5.42	37.47	1.14
i	2.37	-12.507	555		567		-22.275	-34.782	-17.35	0.33	-5.21	36.02	1.27
j	2.35	-12.461	555		570		-21.944	-34.346	-17.13	0.32	-5.14	35.56	1.26
k	2.15	-11.341	555		555		-23.594	-34.842	-17.83	0.30	-5.23	36.18	1.15
l	2.72	-11.715	555		564		-22.605	-34.320	-17.12	0.31	-5.14	35.64	1.19
m	1.91	-10.079	555		546	0.217	-24.527	-34.906	-17.41	0.26	-5.22	36.14	1.02
n	3.125	-16.491	70	0.177	70	0.180	0	-16.491	-8.22	0.13	-2.47	17.08	1.67
o	0.315	-1.662	70	0.177	96	0.185	1.479	-0.173	-0.09	0.04	-0.03	0.14	0.17
p	2.5	-13.193	400	0.185	400	0.212	-16.773	-29.966	-14.95	0.35	-4.89	31.03	1.34
q	2.5	-13.193	400	0.185	384	0.211	-18.145	-31.278	-15.90	0.35	-4.77	33.01	1.34
r	2.35	-12.407	555	0.186	549	0.217	-24.497	-36.900	-18.41	0.32	-5.52	38.21	1.26
s	2.150	-11.346	555		561	0.218	-22.936	-34.782	-17.10	0.30	-5.13	35.50	1.15
t	2.25	-11.873	555		522	0.217	-27.457	-37.350	-19.62	0.31	-5.29	40.73	1.20
u	2.76	-14.565	555		585	0.218	-20.293	-34.358	-17.39	0.38	-5.22	36.99	1.42
v	2.12	-11.187	555		586	0.219	-18.817	-30.004	-16.97	0.39	-4.89	31.07	1.13
w	1.44	-7.599	555		556	0.218	-24.147	-31.746	-15.84	0.20	-4.25	31.57	0.77
x	0.3	-15.93	547		430	0.215	-36.996	-38.579	-19.25	0.04	-5.77	30.95	0.16
y	1.7	-3.694	547		550	0.209	-16.167	-19.161	-24.87	0.10	-7.46	51.63	0.37

COMBUSTION ENGINEERING, INC.

ENGINEERING DEPARTMENT, CHATTANOOGA, TENN.

NUMBER 5-204-P | A 553

SHEET 13 OF 15

CHARGE NO. _____

DATE _____ BY SCARRELL

DESCRIPTION STRUCTURAL AND FATIGUE ANALYSIS OF
BOTTOM HEAD

CHECK DATE _____ BY _____

5. DETAILED ANALYSIS:

f. STRESSES:

$$S_{max} = \sigma_1 - \sigma_2 = 0.95 - (-44.20) = 55.15 \text{ ksi} < 3S_u = 62.0 \text{ ksi}$$

FOR LOC 700-1

TRANSIENT	POINT-1							POINT-2						
	σ_1	σ_2	σ_3	$\sigma_1 - \sigma_2$	$\sigma_1 - \sigma_3$	$\sigma_2 - \sigma_3$	σ_1	σ_2	σ_3	$\sigma_1 - \sigma_2$	$\sigma_1 - \sigma_3$	$\sigma_2 - \sigma_3$	$\sigma_1 - \sigma_3$	
a	0	0.04	-0.91	-0.32	0.95	0.36	-0.59	0.04	-0.91	0	0.95	1.04	-0.91	-3.61
1.17ms	-15.01	29.41	-2.25	-43.42	-12.76	30.66	15.63	37.61		-21.98	15.12	37.61	150.44	
STRESS RATE	-17.31	32.49	-2.25	-49.79	-15.06	34.73	17.93	43.06		-25.13	17.93	43.06	172.24	
b	0	-18.70	35.30	-7.25	-54.20	-16.65	37.55	19.52	46.32		-27.30	19.52	46.32	187.28
1.17ms	-2.99	5.54	-0.32	-6.53	-2.67	5.86	3.01	7.36		-4.29	3.01	7.36	29.44	
c	20 min	-16.75	31.49	-2.25	-48.24	-14.50	33.74	17.37	41.73		-24.36	17.37	41.73	166.92
d	20 min	-17.24	32.61	-2.25	-51.55	-15.69	35.26	18.56	44.57		-26.01	18.56	44.57	178.28
e	100sec	-18.41	34.37	-2.12	-52.78	-16.27	36.51	19.01	45.59		-26.58	19.01	45.59	182.36
25sec	-18.26	34.20	-2.29	-52.46	-15.98	36.42	18.82	45.54		-26.46	18.82	45.54	181.36	
f	40sec	-17.64	33.12	-2.32	-50.76	-15.32	35.40	18.28	43.90		-25.62	18.28	43.90	175.60
100sec	-17.27	32.42	-2.26	-49.70	-15.01	34.69	17.89	42.97		-25.08	17.89	42.97	171.88	
260sec	-17.75	33.19	-2.14	-50.94	-15.61	35.33	18.29	44.03		-25.69	18.35	44.03	176.12	
g	2 min	-17.02	32.00	-2.37	-49.10	-14.63	34.45	17.68	42.50		-24.82	17.68	42.50	170.00
3.2 min	-16.81	31.68	-2.35	-48.49	-14.46	34.03	17.45	41.96		-24.51	17.45	41.96	167.84	
10.4 min	-17.13	32.10	-2.25	-49.23	-14.98	34.25	17.73	42.56		-24.83	17.73	42.56	170.24	
h	10 sec	-16.81	31.59	-2.22	-48.40	-14.59	33.21	17.43	41.87		-24.44	17.43	41.87	167.48
65 sec	-17.15	31.94	-1.91	-49.09	-15.24	33.85	17.61	42.32		-24.71	17.67	42.32	169.52	
i	200 min	-7.79	14.18	-2.13	-73.97	-4.66	19.31	8.65	21.12		-12.47	8.65	21.12	84.45
0.1 sec	-0.05	3.23	-0.32	-0.38	0.27	0.45	0.13	0.39		-0.26	0.13	0.39	1.56	
5 ms	-14.60	27.89	-2.50	-42.49	-12.10	30.39	15.30	36.85		-21.55	15.30	36.85	147.4	
2 ms	-15.55	29.58	-2.51	-45.13	-13.05	32.08	16.25	39.12		-22.87	16.25	39.12	156.48	
k	~	-18.24	35.95	-2.35	-52.04	-15.74	36.20	18.73	44.99		-26.26	18.73	44.99	179.96
~	-16.80	31.52	-2.15	-48.32	-14.65	33.67	17.40	41.78		-24.38	17.40	41.78	167.12	
l	175 sec	-19.31	36.04	-2.25	-55.35	-17.06	38.29	19.93	47.82		-27.89	19.93	47.82	191.28
m	105 sec	-17.01	32.35	-2.76	-49.36	-14.25	35.11	17.77	42.79		-25.02	17.77	42.79	171.16
29 sec	-14.68	27.71	-2.12	-42.89	-12.56	29.83	15.26	36.69		-21.03	15.26	36.69	146.76	
145 sec	-15.64	29.89	-1.44	-44.53	-14.20	30.33	16.04	38.39		-22.35	16.04	38.39	153.56	
n	33 sec	-19.21	34.34	-0.80	-53.55	-18.91	34.64	19.29	45.88		-26.59	19.29	45.88	183.52
54 sec	-24.77	44.54	-0.70	-69.31	-24.07	45.24	24.97	59.46		-34.49	24.97	59.46	237.84	

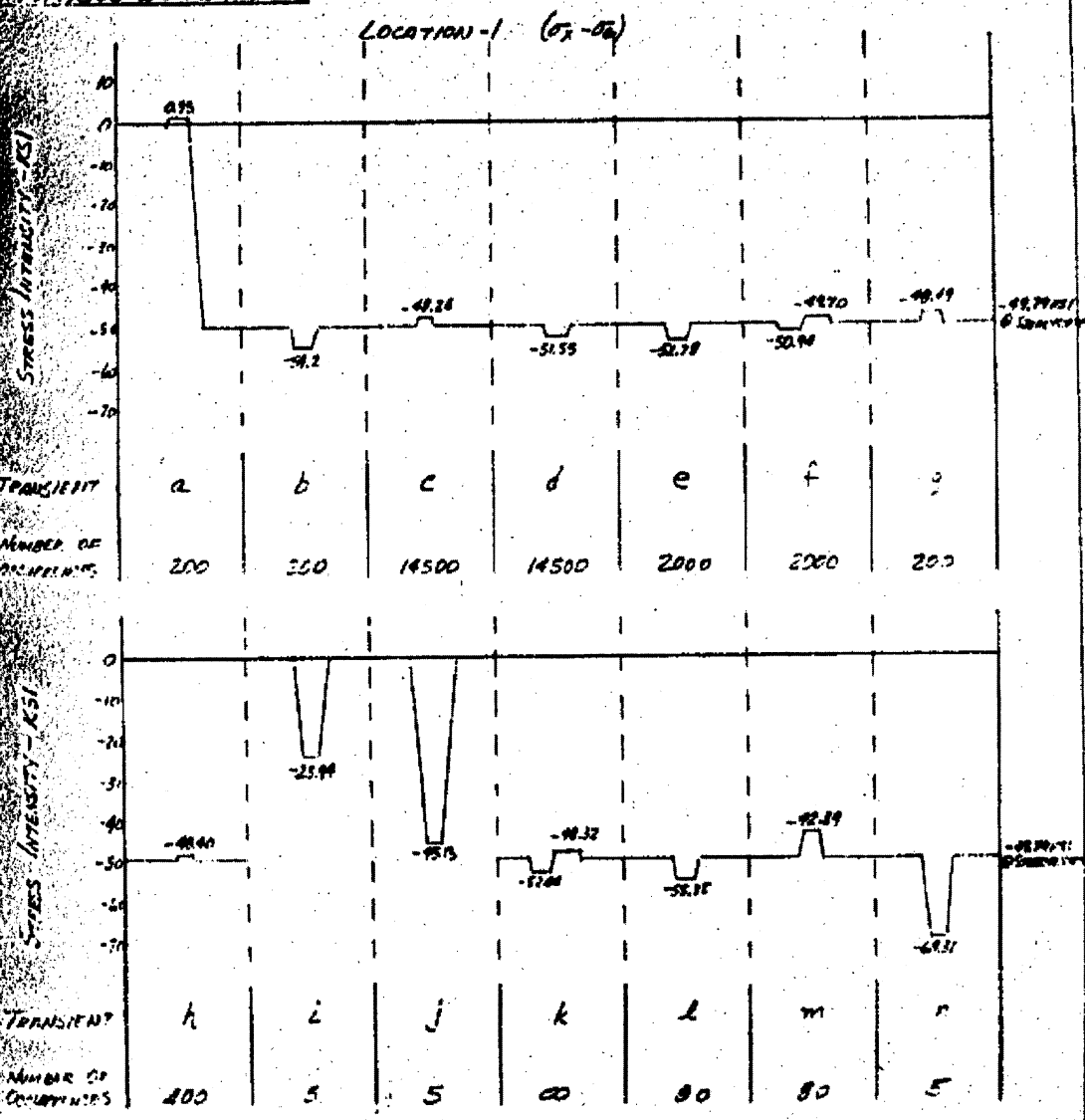
COMBUSTION ENGINEERING, INC.
 ENGINEERING DEPARTMENT, CHATTANOOGA, TENN.

NUMBER 5-201-P | A 354
 SHEET 14 OF 15
 DATE _____ BY DOCKELL
 CHECK DATE _____ BY _____

CHARGE NO. _____
 DESCRIPTION STRUCTURAL AND FATIGUE ANALYSIS OF
BOYTON HEAD INSTRUMENTATION POINTS

5- DETAILED ANALYSIS:

FATIGUE EVALUATION:



Stress	S_{max}	S_{min}	NUMBER OF CYCLES	N^a	U	* From Fig. 11-40(b) of Ref. 1
0.95	-49.31	35.13	5	145000	0.00008	
0.95	-55.35	28.75	80	560000	0.00014	
0.95	-54.20	27.58	115	660000	0.00017	$U_{total} = 0.00025$
0	-45.13	22.57	5	∞	0	

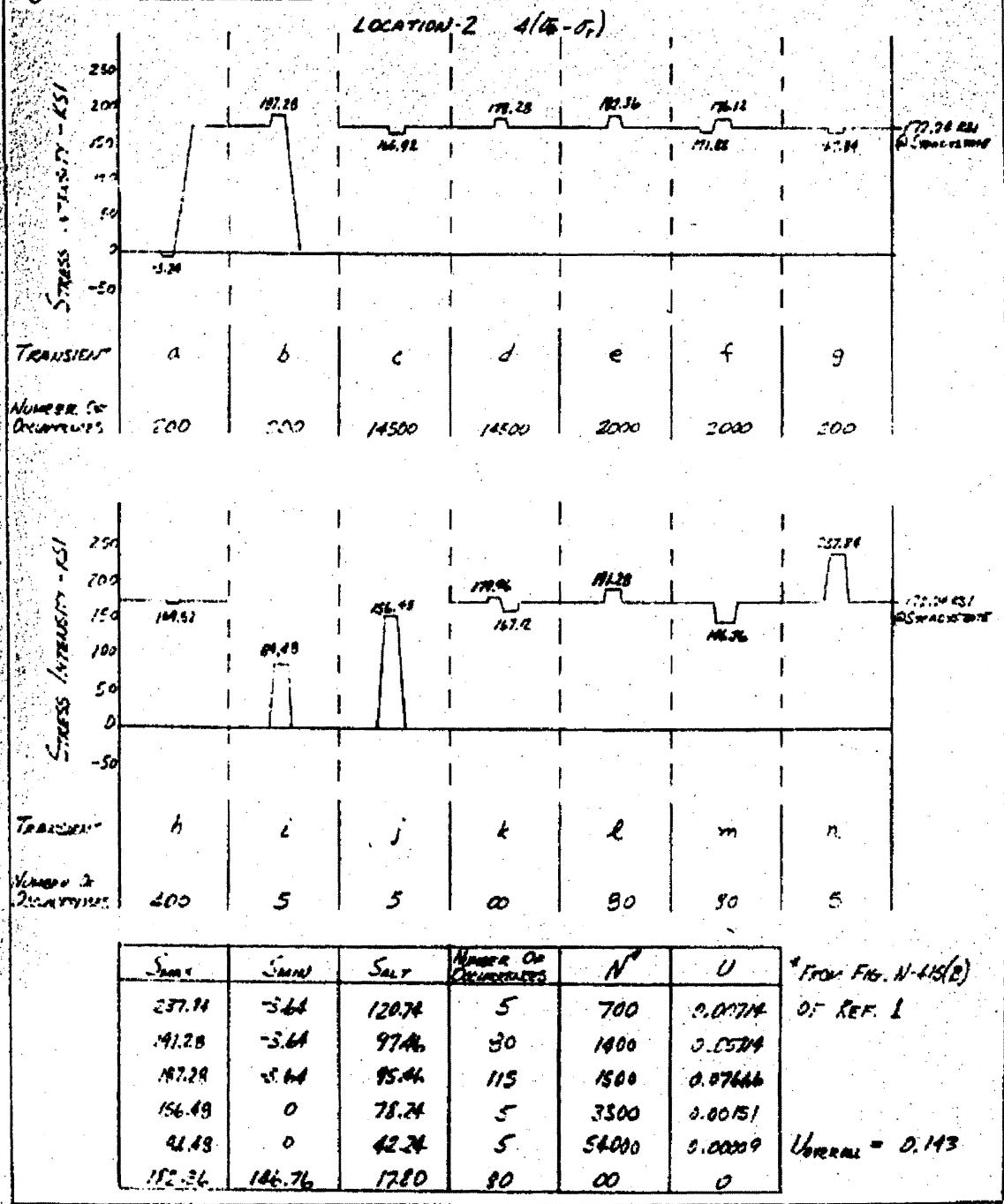
COMBUSTION ENGINEERING, INC.
ENGINEERING DEPARTMENT, CHATTANOOGA, TENN.

NUMBER 5-201-P | A 355
SHEET 15 OF 15
DATE _____ BY COOPER
CHECK DATE _____ BY _____

CHARGE NO. _____
DESCRIPTION STRUCTURAL AND FATIGUE ANALYSIS OF
BOTTOM HEAD INSTRUMENTATION PENETRATIONS

5. DETAILED ANALYSIS:

3. FATIGUE EVALUATION:



A-356

NOTATION

- ν - Poisson's ratio - taken to be 0.3
- E - Elastic modulus (lbs/in²)
- α - Coefficient of thermal expansion (in/in/°F)
- P - Pressure (lbs/in²)
- W - Resultant axial force at any transverse cross-section (lbs)
- T - Temperature (°F or as specified)
- V - Axial component of unit edge force (lbs/in)
- H - Radial component (perpendicular to X-axis) of unit edge force (lbs/in)
- M - Unit bending moment (in-lbs/in)
- $\Delta \delta$ - Components of deflection normal to the X-axis; radial deflection; (positive outward) where Δ results from the action of redundant forces and δ results from all other causes (in)
- $\Delta^* \delta^*$ - Components of rotation (positive if radial deflections of successive adjacent points toward the positive X direction are increasing) where Δ^* results from the action of redundant forces and δ^* results from all other causes (radians)
- X - Axis of revolution
- R - A radial distance measured normal to the axis of revolution (in)
- t - Shell thickness as measured normal to the mid-surface (in)
- σ - Normal stress; the subscripts x , θ and r denote meridional, circumferential, and radial (or lateral) stresses, respectively (lbs/in²)
- ϵ - Strain - Elongation per unit length (in/in)

APPENDIX B

THERMAL ANALYSIS

B-1

APPENDIX B
THERMAL ANALYSIS
TABLE OF CONTENTS

	<u>Page</u>
B.1.0 INTRODUCTION	B-2
B.2.0 NOMENCLATURE	B-2
B.3.0 GENERAL SOLUTIONS	B-3
B.3.1 Transient and Steady State - One, Two or Three Dimensional	B-3
B.3.2 Transient - One Dimensional	B-5
B.3.3 Transient - One Dimensional	B-7
B.3.4 Transient - One Dimensional	B-8
B.3.5 Steady State - One Dimensional - Heat Generation	B-10
B.3.6 Thermal Moment	B-12
B.3.7 Material Properties & Film Coefficients	B-12
B.4.0 APPLICATION OF GENERAL METHODS OF SOLUTION AND RESULTS AT SPECIFIC LOCATIONS	B-14
B.4.1 Head and Vessel Flanges	B-14
B.4.2 Inlet Nozzle	B-16
B.4.3 Outlet Nozzle	B-17
B.4.4 Closure Head	B-19
B.4.5 Vessel Wall	B-19
B.4.6 Bottom Head	B-19
B.4.7 Vessel Supports	B-20
B.5.0 REFERENCES	B-21
B.6.0 DETAILED RESULTS	B-22

B-1.0 INTRODUCTION

This appendix presents a summary of the thermal analysis of the Indian Point, Plant #3 Pressurized Water Reactor Vessel. The assumptions made, method of analysis and results of the investigations are presented. Temperature distributions obtained from two-dimensional heat flow analyses are presented on cross sections of the components considered. Results of the one-dimensional heat flow analyses are presented in the form of graphs. The times for which distributions are presented were selected to present the total effects of the transients.

B-2.0 NOMENCLATURE

- a - Actual thickness of clad material, ft
- A - Cross section area, ft²
- b - Dimension, ft
- C_j - Thermal capacitance of node j, BTU/°F
- c_p - Specific heat, BTU/lb-°F
- c - Actual thickness of base metal, ft
- d - Equivalent thickness of clad material, ft
- E - Modulus of elasticity, psi
- g - Acceleration of gravity, ft/sec²
- h - Heat transfer coefficient, BTU/hr-ft²-°F
- k - Thermal conductivity, BTU/hr-ft-°F
- L - Length along a heat flow path, ft
- m - Slope of temperature vs time curve, °F/hr
- N_{F0} - Fourier modulus, dimensionless
- p - Slope of temperature vs time curve at x=0, °F/hr
- q - Rate of heat flow, BTU/hr
- q_j - Heat generation of the node j, BTU/hr
- q''' - Rate of heat generation per unit volume, BTU/hr-ft³
- q₀''' - Rate of heat generation per unit volume at the surface, BTU/hr-ft³
- r - Dimension, ft
- R - Thermal resistance, hr-°F/BTU
- T - Temperature, °F
- T₀ - Uniform initial temperature, °F
- T₁ - Temperature at x=b, °F
- ΔT - Temperature difference, °F
- u - Slope of temperature vs time curve at x=b, °F/hr
- V - Volume, ft³
- x - Dimension, ft
- α - Thermal diffusivity, ft²/hr
- α' - Coefficient of thermal expansion, ft/ft-°F

- B - Linear absorption coefficient for heat generation, $1/ft$
 ϵ - Emissivity for radiation, ft^2/hr
 θ - $T-T_0$, Temperature change, $^{\circ}F$
 μ - Absolute viscosity, $lb/ft-hr$
 ν - Poisson's ratio, dimensionless
 ξ - $\frac{x}{b}$, distance ratio, dimensionless
 ρ - Density, lb/ft^3
 σ - Thermal stress, psi
 τ - Time, hr
 $\Delta\tau$ - Time difference, hr
 φ - $\frac{\Delta T}{b^2}$, temperature ratio, dimensionless
 ψ - Natural convection property function, $1/ft^3 \text{ } ^{\circ}F$

B.3.0 GENERAL SOLUTIONS

Various procedures were used to determine the thermal information presented in this appendix. The following paragraphs describe the techniques used and the conditions under which each would be applicable.

- B.3.1 Transient and steady state temperature distributions determined by use of a finite difference method programmed for solution on a digital computer.

A code has been written which makes use of the general heat balance equations derived by Hellman, Habetler, and Babrov (1). Through the use of this code, temperature distributions can be obtained in bodies having irregular geometries and composed of different materials.

The object being investigated is divided into a system of blocks or nodes. The thermal capacitance of each node and the thermal resistance between nodes is calculated using the physical properties of the material.

The thermal capacitance of node j is:

$$C_j = \rho c_p V_j$$

The thermal resistance between homogeneous nodes j and i is:

$${}_jR_i = \frac{{}_jL_i}{k_j A_i}$$

B-4

where jL_1 is the length of the heat flow path between nodes j and i , jA_1 is the area normal to jL_1 and common to both nodes, k is the thermal conductivity of the material.

The thermal resistance between non-homogeneous nodes j and i in series is:

$$jR_1 = \frac{j(L_1)_1}{k_1 j(A_1)_1} + \frac{j(L_2)_1}{k_2 j(A_2)_1} + \dots + \frac{j(L_n)_1}{k_n j(A_n)_1}$$

The thermal resistance for a film is:

$$jR_1 = \frac{1}{h jA_1}$$

The equation for the change in temperature of a particular node in the time $\Delta\tau$ is:

$$\Delta T = \frac{\Delta\tau}{C_j} [q(\text{conducted}) + q(\text{generated})]$$

The rate at which heat is conducted into the node is:

$$q = \sum_{i=1}^n \frac{T_i - T_j}{jR_1}$$

where i represents each bordering node and jR_1 is the thermal resistance between the i node and the node under consideration.

Thus, the equation for the change in temperature of a particular node becomes:

$$\Delta T_j = \frac{\Delta\tau}{C_j} \left[\sum_{i=1}^n \frac{T_i - T_j}{jR_1} + q_j \right]$$

The temperature of each node is calculated at successive time intervals through the use of the finite difference equation:

$$T(\tau + \Delta\tau) = T_\tau + \Delta T$$

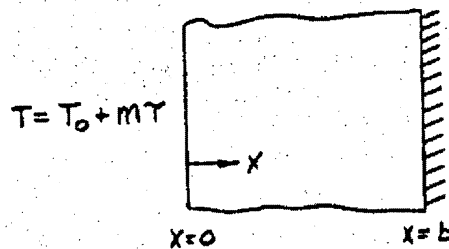
where ΔT is obtained from the previous equation and evaluated at time τ .

For a steady state problem, the term in brackets must be equal to zero; hence,

$$T_j = \frac{\sum_{i=1}^n \frac{1}{R_{j,i}} T_i + q_j}{\sum_{i=1}^n \frac{1}{R_{j,i}}}$$

This expression is equivalent to performing a heat balance about node j .

- B.3.2 Transient solution for a finite slab in which one boundary has a linear temperature change, while the other boundary is insulated. Initially the slab is isothermal.



Assumptions:

1. One-dimensional heat flow.
2. Thermal properties of the material do not vary with temperature and may be evaluated at the average temperature over the range covered.
3. Infinite heat transfer coefficient at $x=0$.

Mathematical statement of the problem:

$$\frac{\partial^2 T}{\partial x^2} - \frac{1}{\alpha} \frac{\partial T}{\partial \tau} = 0 \quad \text{for } 0 < x < b, \tau > 0$$

Boundary conditions:

$$T = T_0 \quad \text{at } \tau = 0 \quad \text{for } 0 < x < b$$

B-6

$$\frac{dT}{dx} = 0 \text{ at } x=b \text{ for } \tau > 0$$

$$T = T_0 + m\tau \text{ at } x=0 \text{ for } \tau > 0$$

The solution is:

$$T = T_0 + \varphi m \tau$$

where,

$$\varphi = \frac{1}{N_{Fo}} \left[N_{Fo} - \xi \left(1 - \frac{\xi}{2}\right) + \frac{2}{\pi^3} \sum_{n=0}^{\infty} \frac{e^{-(n+\frac{1}{2})^2 \pi^2 N_{Fo}}}{(n+\frac{1}{2})^3} \sin(n+\frac{1}{2})\pi\xi \right]$$

$$T_{\text{mean}} = \frac{1}{b} \int_0^b T \, dx$$

$$T_{\text{mean}} = \frac{1}{b} \int_0^b (T_0 + \varphi m \tau) \, dx$$

$$T_{\text{mean}} = T_0 + \frac{m\tau}{b} \int_0^b \varphi \, dx = T_0 + \varphi_{\text{mean}} m \tau$$

where,

$$\varphi_{\text{mean}} = \frac{1}{N_{Fo}} \left[N_{Fo} - \frac{5}{6} + \frac{2}{\pi^4} \sum_{n=0}^{\infty} \frac{e^{-(n+\frac{1}{2})^2 \pi^2 N_{Fo}}}{(n+\frac{1}{2})^4} \right]$$

This solution only considers slabs of one material. To include clad on the base metal, an equivalent thickness must be added to be base metal thickness.

The equation for the equivalent thickness of clad is:

$$d = -c + \sqrt{c^2 + \frac{a^2 \alpha_2}{\alpha_1} + \frac{2k_2 a c}{k_1}}$$

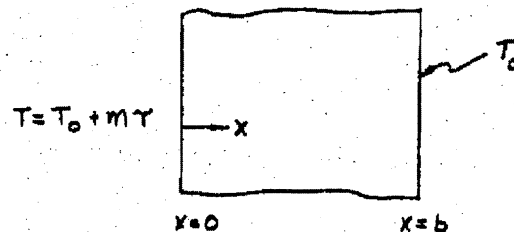
where,

- d = equivalent thickness of clad material
- c = actual thickness of base material
- a = actual thickness of clad material
- α_1 and k_1 = diffusivity and conductivity of clad
- α_2 and k_2 = diffusivity and conductivity of base metal

The slab thickness "b" now becomes (d+c)

The final graph of temperature vs distance can be plotted using (d+c) as the total length. The temperatures in the section $d < x < (d+c)$ are correct for the base metal. However, the temperature distribution from $0 < x < d$ must be "foreshortened" and replotted from $0 < x < a$ where the temperature at $x=a$ is the temperature calculated for $x=d$.

- B.3.3 Transient solution for a finite slab with uniform initial temperature in which one boundary has a linear temperature change while the other boundary is kept at zero temperature.



Assumptions:

1. One-dimensional heat flow.
2. Thermal properties of the material do not vary with temperature and can be evaluated at the average temperature over the range covered.
3. Infinite heat transfer coefficient at $x=0$.

Mathematical statement of the problem:

$$\frac{\partial^2 T}{\partial x^2} - \frac{1}{\alpha} \frac{\partial T}{\partial \tau} = 0 \quad \text{for } 0 < x < b \quad \text{and } \tau > 0$$

B-2

Boundary conditions:

$$T = T_0 \text{ at } \tau=0 \text{ for } 0 < x < b$$

$$\theta = 0 \text{ at } x=b$$

$$T = T_0 + m\tau \text{ at } x=0 \text{ for } \tau > 0$$

The solution is:

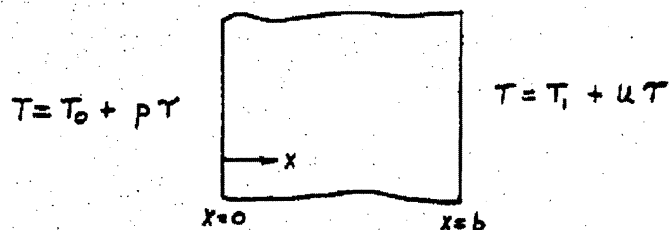
$$T = T_0 + \varphi m \tau$$

where,

$$\varphi = \frac{\theta}{m\tau} = \frac{1}{N_{Fo}} \left\{ \frac{(1-\xi)[6N_{Fo} - \xi(2-\xi)]}{6} + \frac{2}{\pi^3} \sum_{n=1}^{\infty} \frac{e^{-n^2\pi^2 N_{Fo}}}{n^3} \sin n\pi\xi \right\}$$

$$T_{\text{mean}} = \frac{1}{b} \int_0^b (T + \varphi m \tau) dx$$

B:3.4 Transient solution for a finite slab with non-uniform initial temperature which undergoes a linear temperature change on each surface.



Assumptions:

1. One-dimensional heat flow
2. Thermal properties of the material do not vary with temperature and can be evaluated at the average temperature over the range covered.
3. Infinite heat transfer coefficient at $x=0$.
4. $u=0$ forcing the surface at $x=b$ to remain at T_1 .

Mathematical statement of the problem:

$$\frac{\partial^2 T}{\partial x^2} - \frac{1}{\alpha} \frac{\partial T}{\partial \tau} = 0 \text{ for } 0 < x < b \text{ and } \tau > 0$$

Boundary conditions:

$$T = f(x) \text{ at } \tau=0 \text{ for } 0 < x < b$$

$$T = T_0 + p\tau \text{ at } x=0 \text{ for } \tau > 0$$

$$T = T_1 + u\tau \text{ at } x=b \text{ for } \tau > 0, \text{ but } u=0$$

$$\text{so } T = T_1 \text{ at } x=b$$

The solution is:

$$T = \frac{2}{b} \sum_{n=1}^{\infty} e^{\frac{-n^2\pi^2\tau}{b^2}} \sin \frac{n\pi x}{b} \left\{ \int_0^b f(x) \sin \frac{n\pi x}{b} dx \dots \right. \\ \left. + \frac{n\pi a}{b} \int_0^{\tau} e^{\frac{-an^2\pi^2\tau}{b^2}} \left[p\tau T_0 - (-1)^n u\tau T_0 \right] d\tau \right\}$$

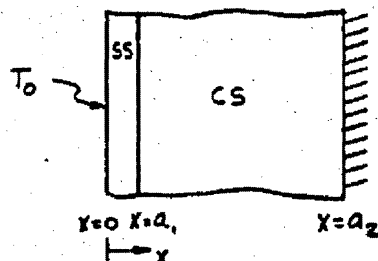
If $f(x) = T_0 + \frac{x}{b} (T_1 - T_0)$ the solution becomes

$$T = p\tau + \tau(u-p)\xi + \frac{b^2}{a} \left[(u-p)\frac{\xi^3}{6} + p\frac{\xi^2}{2} - (u+2p)\frac{\xi}{6} \right] \\ + \frac{2}{b} \sum_{n=1}^{\infty} e^{\frac{-an^2\pi^2\tau}{b^2}} \left[\frac{b}{n\pi} (T_0 - T_1) (-1)^n \sin n\pi\xi \right] \\ - \frac{2}{\pi} \sum_{n=1}^{\infty} e^{\frac{-an^2\pi^2\tau}{b^2}} \left[(T_0 - T_1) (-1)^n \right] \sin n\pi\xi \\ + \frac{2b^2}{\pi^3 a} \sum_{n=1}^{\infty} \left[p + (-1)^n u \right] \frac{e^{\frac{-an^2\pi^2\tau}{b^2}}}{n^3} \sin n\pi\xi$$

The equation for the mean temperature is:

$$T_{\text{mean}} = \frac{1}{b} \int_0^b T \, dx$$

- B.3.5 Nonlinear gradient at steady state resulting from heat generation due to gamma ray capture in a two material finite slab with one surface at a fixed temperature and the other surface perfectly insulated.



Assumptions:

1. One-dimensional heat flow.
2. Thermal properties of the materials do not vary with temperature and can be evaluated at the mean temperature of the body in question.
3. No contact resistance at the junction of the two materials.
4. Heat generation of the form $q''' = q_0''' e^{-\beta x}$.

Mathematical statement of the problem:

$$-k_{ss} \frac{d^2 T_{ss}}{dx^2} = q_0''' e^{-\beta x} \quad \text{for } 0 < x < a_1$$

$$-k_{cs} \frac{d^2 T_{cs}}{dx^2} = q_0''' e^{-\beta x} \quad \text{for } a_1 < x < a_2$$

Boundary conditions:

$$T_{ss} = T_0 \quad \text{at } x=0$$

$$-k_{ss} \frac{dT_{ss}}{dx} = -k_{cs} \frac{dT_{cs}}{dx} \quad \text{at } x=a_1$$

$$T_{ss} = T_{cs} \text{ at } x=a_1$$

$$\frac{dT_{cs}}{dx} = 0 \text{ at } x=a_2$$

The solution is:

$$T_{ss} = \frac{q_0'''}{\beta k_{ss}} \left[\frac{1}{\beta} - \frac{e^{-\beta x}}{\beta} - xe^{-\beta a_2} \right] + T_0$$

$$T_{cs} = \frac{q_0'''}{\beta k_{cs}} \left[a_1 e^{-\beta a_2} + \frac{e^{-\beta a_1}}{\beta} - \frac{e^{-\beta x}}{\beta} - xe^{-\beta a_2} \right]$$

$$+ \frac{q_0'''}{\beta k_{ss}} \left[\frac{1}{\beta} - \frac{e^{-\beta a_1}}{\beta} - a_1 e^{-\beta a_2} \right] + T_0$$

Tangential thermal stresses at $x=a_1$ and $x=a_2$ due to this temperature distribution in a thin walled cylinder with ends free to expand axially but restrained from bending are:

$$\sigma_1 = \left(\frac{E\alpha'}{1-\nu} \right) \left(\frac{q_0'''}{k_{cs}\beta} \right) \left\{ e^{-\beta a_1} \left[\frac{1}{\beta} - \frac{1}{\beta^2(a_2-a_1)} \right] + e^{-\beta a_2} \left[\frac{1}{\beta^2(a_2-a_1)} - \frac{a_2-a_1}{2} \right] \right\}$$

$$\sigma_2 = \left(\frac{E\alpha'}{1-\nu} \right) \left(\frac{q_0'''}{k_{cs}\beta} \right) \left\{ \frac{e^{-\beta a_1}}{\beta^2(a_2-a_1)} - e^{-\beta a_2} \left[\frac{1}{\beta^2(a_2-a_1)} + \frac{1}{\beta} + \frac{a_2-a_1}{2} \right] \right\}$$

where:

- σ_1 = Tangential thermal stress at $x=a_1$
- σ_2 = Tangential thermal stress at $x=a_2$
- E = Modulus of elasticity
- ν = Poisson's ratio
- α' = Linear coefficient of thermal expansion

B.3.6 Thermal moment: A term used in the structural analysis generally at locations of discontinuity where cuts are taken. The moment is due to a radial temperature gradient and is defined mathematically as:

$$M_T = \frac{E\alpha'}{1-\nu} \int_a^b T (R-r)d(R-r)$$

The equation for the mean temperature at a cut through a cylindrical section is:

$$T_M = \frac{2}{b^2-a^2} \int_a^b T r dr$$

where,

- a = Dimension to inside surface
- b = Dimension to outside surface
- r = Dimension ($a < r < b$)
- R = Mean radius
- α' = Coefficient of thermal expansion
- ν = Poisson's ratio

B.3.7 Material Properties and Film Coefficients:

Properties of materials used in this appendix are presented below. All were evaluated at 325°F.

Stainless Steel

$$\begin{aligned} k &= 9.8 \text{ Btu/hr-ft-}^\circ\text{F} \\ \rho &= 495 \text{ lb/ft}^3 \\ c_p &= .127 \text{ Btu/lb-}^\circ\text{F} \end{aligned}$$

Air

$$\begin{aligned} k &= .0204 \text{ Btu/hr-ft-}^\circ\text{F} \\ \nu &= 3.0 \times 10^5 \end{aligned}$$

Carbon Steel

$$\begin{aligned} k &= 26.2 \text{ Btu/hr-ft-}^\circ\text{F} \\ \rho &= 490 \text{ lb/ft}^3 \\ c_p &= .12 \text{ Btu/lb-}^\circ\text{F} \end{aligned}$$

Water

$$\begin{aligned} k &= .40 \text{ Btu/hr-ft-}^\circ\text{F} \\ \nu &= 4.7 \times 10^9 \end{aligned}$$

The following equations were used to calculate the heat transfer coefficients used in the analysis of the head and vessel flanges.

Convection film coefficient in a vertically enclosed gap:

$$\frac{h_c x}{k} = \frac{0.071}{(L/x)^{\frac{1}{5}}} \left[\frac{x^3 \rho^2 g \beta \Delta T}{\mu^2} \left(\frac{c_p \mu}{k} \right) \right]^{\frac{1}{3}}$$

$$h_c = \frac{0.071 k}{(L/x)^{\frac{1}{5}}} [\psi \Delta T]^{\frac{1}{3}}$$

where,

$$\psi = \frac{\rho^2 g \beta}{\mu^2} \left(\frac{c_p \mu}{k} \right)$$

Convection film coefficient in a horizontal enclosed gap:

$$\frac{h_c x}{k} = 0.075 \left[\frac{x^3 \rho^2 g \beta \Delta T}{\mu^2} \left(\frac{c_p \mu}{k} \right) \right]^{\frac{1}{3}}$$

$$h_c = 0.075 k [\psi \Delta T]^{\frac{1}{3}}$$

Convection film off the top of a heated plate:

$$\frac{h_c L}{k} = 0.14 \left[\frac{L^3 \rho^2 g \beta \Delta T}{\mu^2} \left(\frac{c_p \mu}{k} \right) \right]^{\frac{1}{3}}$$

$$h_c = 0.14 k [\Delta T]^{\frac{1}{3}}$$

The convection film coefficient on the bottom side of the same plate is assumed to be half that on the top side.

The equation for the radiation coefficient across the air gaps and off the top and bottom of the refueling plate is as follows:

$$h_r = \frac{0.173 \times 10^{-8} (T_1^4 - T_2^4)}{\frac{1}{\epsilon_1} + \frac{1}{\epsilon_2} - 1} (T_1 - T_2)$$

$$\epsilon_1 = \epsilon_2 = 0.65$$

B.4.0 APPLICATION OF GENERAL SOLUTIONS AND RESULTS AT SPECIFIC LOCATIONS

B.4.1 Head and Vessel Flanges: A representative section of the vessel flange - head flange region was divided into a series of nodes as in Figure B-1 on Page B-23. For calculating node volumes and heat transfer areas, a cylindrical sector with an angle equal to half the angle between two studs was taken. This model considers two dimensional heat flow (axial and radial) except in the head flange where the studs pass through. In this area, a third dimension is considered as heat is transferred between the stud and flange.

Assumptions:

- a. Two-dimensional heat flow.
- b. Heat generation negligible.
- c. Thermal properties do not vary with temperature.
- d. Natural convection is assumed in the gap between the core barrel and vessel flange.
- e. All other surfaces in contact with primary coolant are assumed to have an infinite heat transfer coefficient.
- f. Outside surfaces of flanges, vessel and head are perfectly insulated.
- g. Natural convection and radiation is assumed in the annulus between the stud and head flange and in the gap between the head and vessel flanges.
- h. The refueling plate transfers heat to the surroundings by both radiation and convection.

The head and vessel flanges were analyzed for the following thermal conditions using the method described in B.3.1.

- a. Heatup Transient: Inside surfaces are heated from 100°F to 547°F at a linear rate of 100°F/hr while the ambient condition remains at 120°F.

B-15

- b. Steady State: Inside surfaces are held constant at 547°F and the ambient at 120°F .
- c. Cooldown Transient: The inside surfaces are cooled from 547°F to 100°F at a linear rate of 100°F/hr while the ambient is held at 120°F . The initial condition for this transient is the steady state condition described in b.

Results:

Nodal layouts of the flanges showing temperature distributions at times during heatup and cooldown transients plus steady state are presented in Figures B-1 thru B-9. Figure B-39 is a sketch of the flange region showing the locations of discontinuity where the effects of radial gradients were considered. At these locations, the radial gradients were plotted, and from these gradients values were obtained for the mean temperature at the cut and the thermal moment. The radial gradients are shown in Figures B-40 thru B-49, and the thermal moments resulting from these gradients are tabulated on Page B-100.

Axial gradients in the flanges were also plotted from the temperature distributions at times during heatup, cooldown and at steady state. These gradients are presented in Figures B-78 thru B-83.

For the Plant Hydrostatic Test (2500 psia), the inside surfaces are heated from 100°F to 400°F at 100°F/hr while the plant is being pressurized. During plant depressurization, the inside surfaces are cooled back to 100°F at 100°F/hr . These heatup and cooldown transients are at the same rate but over a shorter range than the normal heatup and cooldown. Therefore, it would be conservative to use the results of normal heatup and cooldown for the hydrostatic test transients.

Other operating transients applied to this region have faster rates than heatup and cooldown, but the range of temperature change is much shorter. Therefore, it was conservative to consider the mean temperature of the body did not change from the initial condition while the temperature of the inside surface followed the fluid transient. Differences between the mean temperature and the inside surface temperature at times during these transients are tabulated on Page B-121.

B-16

B.4.2 Inlet Nozzle: A cross section of the nozzle was divided into a series of nodes as in Figure B-10 on Page B-32. This model, consisting of a cylindrical sector with an angle of one radian, was used to perform a two-dimensional thermal analysis using the technique described in B.3.1 and the following assumptions.

- a. Two-dimensional heat flow.
- b. Heat generation negligible.
- c. Thermal properties do not vary with temperature.
- d. All surfaces in contact with the primary coolant are assumed to have an infinite heat transfer coefficient.
- e. Outside surfaces are perfectly insulated.

Results:

Temperature distributions were obtained for times during a 100°F/hr heatup from 100°F to 547°F . These distributions are shown on nodal layouts in Figures B-10 thru B-13. Figure B-50 shows the locations of discontinuity where the effects of radial gradients were considered. At these locations, the radial gradients were plotted, and from these gradients values were obtained for the mean temperature at the cut and the thermal moment. The radial gradient plots are found in Figures B-51 thru B-55 and the thermal moments are tabulated on Page B-101.

Gradients in the axial direction were also plotted for the nozzle at times during the heatup transient. These plots are found in Figures B-84 and B-85.

Temperature distributions were not obtained for the cooldown transient. Since cooldown is over the same range and at the same rate as heatup, cooldown gradients would simply be mirror images of those for the heatup transient. Also, the values for thermal moments which were obtained for heatup, with signs reversed, can be used for corresponding times during cooldown.

The results of normal heatup and cooldown were used for the hydrostatic test transients as described for the flanges in B.4.1.

At steady state, the nozzle will be isothermal at the inlet coolant temperature since there is no heat sink.

The operating transients for the inlet nozzle were investigated in the same manner as for the flange analysis in Section B.4.1. The results are presented on Page B-122.

- B.4.3 Outlet Nozzle: A representative section of the outlet nozzle was divided into a series of nodes as in Figure B-14 on Page B-36. This model, consisting of a cylindrical sector with an angle of one radian, was used to perform a thermal analysis using the method described in B.3.1.

Assumptions:

- a. Two-dimensional heat flow.
- b. Heat generation negligible.
- c. Thermal properties do not vary with temperature.
- d. All surfaces in contact with the primary coolant are assumed to have an infinite heat transfer coefficient.
- e. Outside surfaces perfectly insulated.

Temperature distributions in the outlet nozzle were obtained for the following transient and steady state conditions.

- a. Heatup: Inside surfaces are heated from 100°F to 547°F at a linear rate of 100°F/hr. Both inlet and outlet fluids follow the same transient.
- b. 100% Power Steady State: The coolant inside the nozzle is held constant at 613°F while the coolant contacting the vessel shell adjacent to the nozzle is held at 555°F.
- c. Operating Transients: Temperature distributions were obtained for operating transients including plant loading and unloading, step reduction from 100% to 50% load, reactor trip from full power, loss of flow, one pump and loss of load. Fluid transients for these cases are found in the Equipment Specification.

Results:

Nodal layouts of the outlet nozzle showing temperature distributions for times during heatup, plant loading, at 100% power steady state and during plant unloading are presented in Figures B-14 thru B-26. Figure B-56

is a sketch of the nozzle showing the locations of discontinuity where effects of radial gradients were considered. At these locations, radial gradients were plotted for the conditions above. From these gradients, values were obtained for the mean temperature at the cut and the thermal moment. The radial gradient plots are found in Figures B-57 thru B-71 and the resulting thermal moments are tabulated on Pages B-102 and B-103.

Axial gradients were also plotted for the nozzle at times during heatup, plant loading at 100% power steady state and during plant unloading. They are found in Figures B-86 thru B-91.

As in the inlet nozzle analysis, the cooldown transient was not completely analyzed. The gradients are mirror images of those for heatup and the thermal moments, with reversed signs, can be used for corresponding times during cooldown.

At zero power steady state, both inlet and outlet fluids are at 547°F. With the outer surface of the nozzle insulated there is no heat sink. Therefore, at this steady state the nozzle will be isothermal at 547°F.

The results of heatup and cooldown were also used for the plant hydrostatic test transients as described for the flange analysis in B.4.1.

Temperature distributions for operating transients including step reduction from 100% to 50% load, reactor trip from full power, loss of flow, one pump and loss of load are presented in Figures B-27 thru B-38. These transients have faster rates than heatup, plant loading and plant unloading, and their effects are only seen a short distance from the surface. In view of this, it was conservative to consider the inside surface follows the fluid temperature and calculate the ΔT between the mean temperature and inside surface temperature. These temperature differences are tabulated on Pages B-123 and B-124.

For the step load transients of $\pm 10\%$ of full power and steam break from hot zero power where both inlet and outlet fluids follow the same transient, the inside surface temperature was assumed to follow the fluid temperature while the mean temperature of the nozzle did

not change from the initial condition. Differences between the mean and surface temperatures are tabulated on Pages B-123 and B-124.

- B.4.4 Closure Head: The vessel closure head was analyzed to determine the mean temperature of the head at the end of the 100°F/hr heatup and cooldown transients between 100°F and 547°F and at the end of the hydrostatic test transients during which the vessel is heated and cooled between 100°F and 400°F at 100°F/hr .

Results of the one-dimensional analytical solution as described in Section B.3.2 showed the mean temperature of the head to be 518°F at the end of heatup and 129°F at the end of cooldown. At the end of the hydro heatup and cooldown transients, the mean temperature of the head is 384°F and 116°F , respectively.

- B.4.5 Vessel wall: The procedure described in B.3.2 was used to perform the one-dimensional analysis of the vessel wall in the nozzle region and in the lower shell region for the heatup and hydro heatup transients.

Temperature distributions for the two wall sections, presented in the form of graphs, for times during heatup and hydro heatup are on pages B-94 thru B-97. Using these curves, the mean temperature and inside and outside surface temperatures were obtained for the times investigated. Differences between the mean temperature and the temperatures of the inside and outside surfaces are tabulated on Page B-104.

The procedure in B.3.5 was used in determining the maximum allowable rate of gamma heating in the thinner section of the vessel wall. This rate was calculated by substituting $2 S_m$ for α_1 in the equation for thermal stress at $x=a_1$ and solving for q_0''' . With $B = 0.4 \text{ in}^{-1}$ and $2 S_m = 53,400 \text{ psi}$, the maximum value of q_0''' was determined to be $164,000 \text{ Btu/ft}^3\text{-hr}$.

- B.4.6 Bottom Head: The method in B.3.2 was also used to determine the mean, inside surface and outside surface temperatures in the bottom head at times during the heatup and hydro heatup transients. Differences between the mean temperature and the temperatures of the inside and outside surfaces during these transients are presented on Page B-105.

B-20

B.4.7 Vessel Supports: The vessel is supported off the nozzles. Four nozzles, two inlet and two outlet, are used in the support arrangement. These nozzles have integral pads built up on the bottom sides and rest on support shoes. The support shoes are attached to a ring girder which rests on a concrete foundation. Although both inlet and outlet nozzles are used for supports, the geometry of the inlet nozzle presents the more severe case and was used for both nozzles in the analysis.

The following transients and steady state conditions were investigated. For all conditions, the back surface is held at 100°F. This temperature represents the temperature at the bottom of the support shoe and is assumed to be equal to the ambient temperature.

- a. Plant Heatup - Inside surface is heated from 100°F to 547°F at a linear rate of 100°F/hr.
- b. Hydro Heatup - Inside surface is heated from 100°F to 400°F at a linear rate of 100°F/Hr.
- c. Steady State - at steady state, the temperature distribution through the nozzle wall and pad is assumed to be linear between the fluid temperature inside the nozzle and 100°F at the bottom of the support shoe.

Inside temperatures for the steady states investigated are:

1. Hydro Steady State - 400°F (inlet and outlet nozzles).
 2. Zero Power Steady State - 547°F (inlet and outlet nozzles).
 3. 100% Power Steady State - 555°F (inlet nozzle only).
 4. 100% Power Steady State - 613° (outlet nozzle only).
- d. Plant Cooldown - Inside surface is cooled from 547°F to 100°F at a linear rate of 100°F/hr. The initial condition for this transient is the zero power steady state distribution.
 - e. Hydro Cooldown - This transient starts from the hydro steady state. The inside surface is cooled from 400°F to 100°F at 100°F/hr. The distribution at the end of hydro cooldown is assumed to be the same as that for the end of plant cooldown.

B-21

The procedure in B.3.3 was used to perform the one-dimensional thermal analysis for plant heatup and hydro heatup. The plant cooldown transient was analyzed using the one-dimensional analytical solution described in B.3.4.

Temperature distributions thru the nozzle wall and pad at the end of plant heatup, hydro heatup and plant cooldown are presented in Figure B-76. Distributions for hydro, zero power and 100% power steady states are presented in Figure B-77. From these distributions temperatures of the inside and outside surfaces and the mean temperature were obtained. The T between the mean temperature and the temperature of the inside and outside surfaces was calculated. These results are presented on Page B-106.

B.5.0 REFERENCES

1. Hellman, Habetler, and Babrov, "Use of Numerical Analysis in Transient Solution of Two Dimensional Heat Transfer Problems with Natural and Forced Convection", ASME Transactions, 1956.
2. McAdams, W. H., Heat Transmission, Third Edition, McGraw-Hill Book Co., New York, 1954.
3. Anthony, M. L., "Temperature Distributions in Slabs with a Linear Temperature Rise at One Surface", General Discussion on Heat Transfer, 1951.
4. Mac Robert, P. M., Spherical Harmonics, 2nd Edition, 1948
5. Westinghouse Equipment Specifications 676245 and 676514.
6. CE Drawing No. E-234-042.
7. CE Drawing No. E-234-043.
8. CE Drawing No. E-234-045.
9. CE Drawing No. E-234-047.
10. CE Drawing No. E-234-049.

B-22

E.O.

DETAILED RESULTS